Two-axis spin squeezing in two cavities

Caifeng Li,[1,2] Jingtao Fan,[1] Lixuan Yu,[3,1,*] Gang Chen,[1,†] Tian-Cai Zhang,[4] and Suotang Jia[1]

[1]*State Key Laboratory of Quantum Optics and Quantum Optics Devices,*
Institute of Laser Spectroscopy, Shanxi University, Taiyuan 030006, China
[2]*Institute of Theoretical Physics, Shanxi University, Taiyuan 030006, P. R. China*
[3]*Department of Physics, Shaoxing University, Shaoxing 312000, China*
[4]*State Key Laboratory of Quantum Optics and Quantum Optics Devices,*
Institute of Opto-Electronics, Shanxi University, Taiyuan 030006, China

Ultracold atoms in an ultrahigh-finesse optical cavity are a powerful platform to produce spin squeezing since photon of cavity mode can induce nonlinear spin-spin interaction and thus generate a one-axis twisting Hamiltonian $H_{\mathrm{OAT}} = qJ_x^2$, whose corresponding maximal squeezing factor scales as $N^{-2/3}$, where N is the atomic number. On the contrary, for the other two-axis twisting Hamiltonian $H_{\mathrm{TAT}} = q(J_x^2 - J_y^2)$, the maximal squeezing factor scales as N^{-1}, approaching the Heisenberg limit. In this paper, inspired by recent experiments of cavity-assisted Raman transitions, we propose a scheme, in which an ensemble of ultracold six-level atoms interacts with two quantized cavity fields and two pairs of Raman lasers, to realize a tunable two-axis spin Hamiltonian $H = q(J_x^2 + \chi J_y^2) + \omega_0 J_z$. For proper parameters, the above one- and two- axis twisting Hamiltonians are recovered, and the scaling of N^{-1} of the maximal squeezing factor can occur naturally. On the other hand, in the two-axis twisting Hamiltonian, spin squeezing is usually reduced when increasing the effective atomic resonant frequency ω_0. Surprisingly, we find that by combined with the dimensionless parameter $\chi(> -1)$, the effective atomic resonant frequency ω_0 can enhance spin squeezing largely. These results are benefit for achieving the required spin squeezing in experiments.

PACS numbers: 42.50.Dv, 42.50.Pq

I. INTRODUCTION

Squeezed spin states, which were firstly introduced by Kitagawa and Ueda [1], are quantum correlated states with reduced fluctuations in one of the collective spin components [2, 3]. Such states have attracted considerable interest because they not only play significant roles in investigating many-body entanglement [4, 5], but also have important applications in atom interferometers and high-precision atom clocks [7, 8]. In general, there are two methods to produce spin squeezing. One is based on a one-axis twisting Hamiltonian $H_{\mathrm{OAT}} = qJ_x^2$, where q is the nonlinear spin-spin interaction strength and J_x is the collective spin operator in the x direction. When the initial state is prepared as $|J_z = -j\rangle$ for $q > 0$ ($|J_z = j\rangle$ for $q < 0$), the maximal squeezing factor for this one-axis twisting Hamiltonian scales as $N^{-2/3}$ [1], where N is the total atomic number and $J = N/2$. On the contrary, for the other two-axis twisting Hamiltonian $H_{\mathrm{TAT}} = q(J_x^2 - J_y^2)$, the maximal squeezing factor scales as N^{-1} with the same initial state [1]. Since the scaling of N^{-1} approaches the Heisenberg limit, implementing the two-axis twisting Hamiltonian in current experimental setups is very important and necessary [9–11]. A proposing scheme is to transform the one-axis twisting Hamiltonian into the two-axis twisting Hamiltonian by applying pulse sequences or continuous driving in the

two-component Bose-Einstein condensates [12–15]. However, the experimental realization of such two-axis twisting Hamiltonian is still challenging.

Ultracold atoms in an ultrahigh-finesse optical cavity are also a powerful platform to produce spin squeezing since photon of cavity mode can induce nonlinear spin-spin interaction and thus generate the required one-axis twisting Hamiltonian [16–23]. Recently, multi-mode cavities [24] have attracted much attention both experimentally and theoretically [25–29]. On one hand, these setups can be used to explore novel physics, such as the spin-orbit-induced anomalous Hall effect [30, 31], the crystallization and frustration [32, 33], the spin glass [34–37], and the gapless Nambu-Goldstone-type mode without rotating-wave approximation [38]. Moreover, two-mode field squeezing [39] and unconditional preparation of a two-mode squeezed state of effective bosonic modes [40] have also been achieved by introducing two cavities. In the present paper, inspired by recent experiments of cavity-assisted Raman transitions [41, 42], we mainly realize a generalized two-axis spin Hamiltonian by two cavities to enhance spin squeezing largely.

When an ensemble of ultracold six-level atoms interacts with two quantized cavity fields and two pairs of Raman lasers, we first realize a two-mode Dicke model. In the dispersive regime, we obtain a generalized two-axis spin Hamiltonian $H = q(J_x^2 + \chi J_y^2) + \omega_0 J_z$, where χ is a dimensionless parameter and ω_0 is an effective atomic resonant frequency. This realized Hamiltonian has a distinct property that the interaction strength q, the dimensionless parameter χ, and the effective atomic resonant frequency ω_0 can be tuned independently. For reason-

able parameters, the one- and two-axis twisting Hamiltonians are recovered. Numerical results reveal that for the standard two-axis twisting Hamiltonian ($\chi = -1$ and $\omega_0 = 0$), the corresponding maximal squeezing factor scales as N^{-1}, as expected. On the other hand, in the two-axis twisting Hamiltonian H_{TAT}, spin squeezing is usually reduced when increasing the effective atomic resonant frequency ω_0. Surprisingly, we find that by combined with the dimensionless parameter $\chi(> -1)$, the effective atomic resonant frequency ω_0 can enhance spin squeezing largely. These results are benefit for achieving the required spin squeezing in experiments.

This paper is organized as follows. Section II is devoted to realizing the generalized two-axis spin Hamiltonian with independently-tunable parameters. Section III is devoted to introducing the spin squeezing factor. Section IV is devoted to numerically investigating the maximal squeezing factor since for the two-axis spin Hamiltonian, analytical results are very hard to be obtained [2]. The parts of Discussions and Conclusions are given in sections V and VI.

II.   MODEL AND HAMILTONIAN

A.   Proposed experimental setup

Motivated by recent experiments of cavity-assisted Raman transitions [41, 42], here we propose a scheme, in which an ensemble of ultracold six-level atoms interacts with two quantized cavity fields and two pairs of Raman lasers [see Fig. 1(a)], to realize a generalized two-axis spin Hamiltonian with independently-tunable parameters. As shown in Fig. 1(b), six levels consist of two stable ground states ($|0\rangle$ and $|1\rangle$) and four excited states ($|r_1\rangle$, $|r_1\rangle$, $|s_1\rangle$, and $|s_2\rangle$). Two independent photon modes, whose creation and annihilation operators are $a^\dagger$ ($b^\dagger$) and a (b), mediate the $|0\rangle \longleftrightarrow |s_1\rangle$ and $|1\rangle \longleftrightarrow |r_1\rangle$ ($|0\rangle \longleftrightarrow |s_2\rangle$ and $|1\rangle \longleftrightarrow |r_2\rangle$) transitions (red and blue solid lines) with atom-photon coupling strengths g_{s_1} (g_{s_2}) and g_{r_1} (g_{r_2}), respectively. Whereas two pairs of Raman lasers govern the other transitions $\{|0\rangle \longleftrightarrow |r_1\rangle,\ |1\rangle \leftrightarrow |s_1\rangle\}$ and $\{|0\rangle \longleftrightarrow |r_2\rangle,\ |1\rangle \leftrightarrow |s_2\rangle\}$ (red and blue dashed lines) with Rabi frequencies $\{\Omega_{r_1}, \Omega_{s_1}\}$ and $\{\Omega_{r2}, \Omega_{s_2}\}$, respectively. $\Delta_{r_{1,2}}$ and $\Delta_{s_{1,2}}$ are the detunings from the excited states.

B.   Total Hamiltonian

The total Hamiltonian illustrated in Fig. 1 can be written as

$$H_{\text{T}} = H_{\text{C}} + H_{\text{A}} + H_{\text{I}}, \tag{1}$$

where

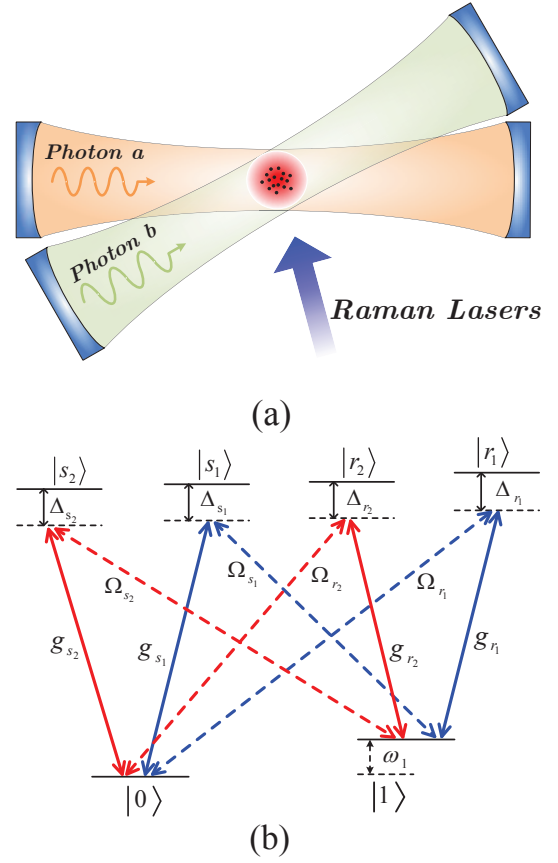$$H_{\text{C}} = \omega_a a^\dagger a + \omega_b b^\dagger b, \tag{2}$$

FIG. 1: (Color online). (a) Proposed experimentally-feasible setup that an ensemble of ultracold six-level atoms interacts with two quantized cavity fields and two pairs of Raman lasers. (b) Energy-level structure and their transitions induced by two photon modes and two pairs of Raman lasers.

$$
\begin{aligned}
H_{\text{A}} = \sum_{j=1}^{N} \Big\{ &\omega_{r_1} |r_1\rangle_j \langle r_1|_j + \omega_{r_2} |r_2\rangle_j \langle r_2|_j + \\
&+ \omega_{s_1} |s_1\rangle_j \langle s_1|_j + \omega_{s_2} |s_2\rangle_j \langle s_2|_j + \omega_1 |1\rangle_j \langle 1|_j \\
&+ \frac{1}{2}\Big[\Omega_{s_1} |s_1\rangle_j \langle 1|_j\, e^{-i(\omega_{1s_1}t - \varphi_{s_1})} \\
&+ \Omega_{s_2} |s_2\rangle_j \langle 1|_j\, e^{-i(\omega_{1s_2}t - \varphi_{s_2})} \\
&+ \Omega_{r_1} |r_1\rangle_j \langle 0|_j\, e^{-i(\omega_{0r_1}t - \varphi_{r_1})} \\
&+ \Omega_{r_2} |r_2\rangle_j \langle 0|_j\, e^{-i(\omega_{0r_2}t - \varphi_{r_2})} + \text{H.c.} \Big] \Big\},
\end{aligned}
\tag{3}
$$

$$
\begin{aligned}
H_{\text{I}} = \sum_{j=1}^{N} \Big[&g_{s_1} |s_1\rangle_j \langle 0|_j\, a + g_{r_1} |r_1\rangle_j \langle 1|_j\, a \\
&+ g_{s_2} |s_2\rangle_j \langle 0|_j\, b + g_{r_2} |r_2\rangle_j \langle 1|_j\, b + \text{H.c.} \Big].
\end{aligned}
\tag{4}
$$

In the Hamiltonians (2)-(4), $\omega_{r_{1,2}}$, $\omega_{s_{1,2}}$, and ω_1 are the atomic frequencies, $\omega_{1s_{1,2}}$ ($\varphi_{s_{1,2}}$) and $\omega_{1r_{1,2}}$ ($\varphi_{r_{1,2}}$) are the frequencies (phases) of Raman lasers, respectively, and H.c. denotes the Hermitian conjugate.

C. Two-mode Dicke model

By means of the Hamiltonian (1), we first realize a two-mode Dicke model with independently-tunable parameters. In the interaction picture with respect to the free Hamiltonian

$$H_0 = \widetilde{\omega_a} a^\dagger a + \widetilde{\omega_b} b^\dagger b + \sum_{j=1}^{N} \left(\widetilde{\omega_{s_1}} |s_1\rangle_j \langle s_1|_j \right. \tag{5}$$

$$+ \widetilde{\omega_{r_1}} |r_1\rangle_j \langle r_1|_j + \widetilde{\omega_{s_2}} |s_2\rangle_j \langle s_2|_j$$

$$+ \widetilde{\omega_{r_2}} |r_2\rangle_j \langle r_2|_j + \widetilde{\omega_1} |1\rangle_j \langle 1|_j \Big),$$

where $\widetilde{\omega_a} = \widetilde{\omega_{s_1}} = (\omega_{0r_1} + \omega_{1s_1})/2$, $\widetilde{\omega_b} = \widetilde{\omega_{s_2}} = (\omega_{0r_2} + \omega_{1s_2})/2$, $\widetilde{\omega_1} = (\omega_{0r_1} - \omega_{1s_1})/2 = (\omega_{0r_2} - \omega_{1s_2})/2$, $\widetilde{\omega_{r_1}} = \widetilde{\omega_1} + \widetilde{\omega_a}$, and $\widetilde{\omega_{r_2}} = \widetilde{\omega_1} + \widetilde{\omega_b}$, the Hamiltonian (1) can be rewritten as

$$\widetilde{H} = \Delta_a a^\dagger a + \Delta_b b^\dagger b + \sum_{j=1}^{N} \Big\{ \Delta_{r_1} |r_1\rangle_j \langle r_1|_j \tag{6}$$

$$+ \Delta_{r_2} |r_2\rangle_j \langle r_2|_j + \Delta_{s_1} |s_1\rangle_j \langle s_1|_j + \Delta_{s_2} |s_2\rangle_j \langle s_2|_j$$

$$+ \Delta_1 |1\rangle_j \langle 1|_j + \frac{1}{2} \Big[\Omega_{s_1} |s_1\rangle_j \langle 1|_j e^{i\varphi_{s_1}}$$

$$+ \Omega_{s_2} |s_2\rangle_j \langle 1|_j e^{i\varphi_{s_2}} + \Omega_{r_1} |r_1\rangle_j \langle 0|_j e^{i\varphi_{r_1}}$$

$$+ \Omega_{r_2} |r_2\rangle_j \langle 0|_j e^{i\varphi_{r_2}} + \text{H.c.} \Big] + \Big[g_{s_1} |s_1\rangle_j \langle 0|_j a$$

$$+ g_{r_1} |r_1\rangle_j \langle 1|_j a + g_{s_2} |s_2\rangle_j \langle 0|_j b$$

$$+ g_{r_2} |r_2\rangle_j \langle 1|_j b + \text{H.c.} \Big] \Big\},$$

where $\Delta_a = \omega_a - \widetilde{\omega_a}$, $\Delta_b = \omega_b - \widetilde{\omega_b}$, $\Delta_{s_1} = \omega_{s_1} - \widetilde{\omega_{s_1}}$, $\Delta_{s_2} = \omega_{s_2} - \widetilde{\omega_{s_2}}$, and $\Delta_1 = \omega_1 - \widetilde{\omega_1}$.

In the large-detuning limit, i.e., $|\Delta_{r_{1,2}, s_{1,2}}| \gg \{\Omega_{r_{1,2}}, \Omega_{s_{1,2}}, g_{r_{1,2}}, g_{s_{1,2}}\}$, all excited states can be eliminated adiabatically [43], and an effective Hamiltonian is obtained by

$$\widetilde{H} = \omega_A a^\dagger a + \omega_B b^\dagger b + \omega_0 J_z + \eta a^\dagger a J_z \tag{7}$$

$$+ \Big[\big(\lambda_{r_1} a e^{-i\varphi_{r_1}} + \lambda_{r_2} b e^{-i\varphi_{r_2}} \big) J_-$$

$$+ \big(\lambda_{s_1} a e^{-i\varphi_{s_1}} + \lambda_{s_2} b e^{-i\varphi_{s_2}} \big) J_+ + \text{H.c.} \Big],$$

where $\eta = g_{r_1}^2/\Delta_{r_1} + g_{r_2}^2/\Delta_{r_2} - g_{s_1}^2/\Delta_{s_1} - g_{s_2}^2/\Delta_{s_2}$, $J_+ = \sum_{j=1}^{j=N} |1\rangle_j \langle 0|_j$, $J_- = \sum_{j=1}^{j=N} |0\rangle_j \langle 1|_j$, and $J_z = \sum_{j=1}^{j=N} (|1\rangle_j \langle 1|_j - |0\rangle_j \langle 0|_j)/2$ are the collective spin operators,

$$\omega_0 = \Delta_1 + \frac{1}{4} \left(\frac{\Omega_{s_1}^2}{\Delta_{s_1}} + \frac{\Omega_{s_2}^2}{\Delta_{s_2}} - \frac{\Omega_{r_1}^2}{\Delta_{r_1}} - \frac{\Omega_{r_2}^2}{\Delta_{r_2}} \right), \tag{8}$$

$$\omega_A = \Delta_a + \frac{1}{2} \left(\frac{N g_{r_1}^2}{\Delta_{r1}} + \frac{N g_{s_1}^2}{\Delta_{s1}} \right), \tag{9}$$

$$\omega_B = \Delta_b + \frac{1}{2} \left(\frac{N g_{r_2}^2}{\Delta_{r_2}} + \frac{N g_{s_2}^2}{\Delta_{s_2}} \right), \tag{10}$$
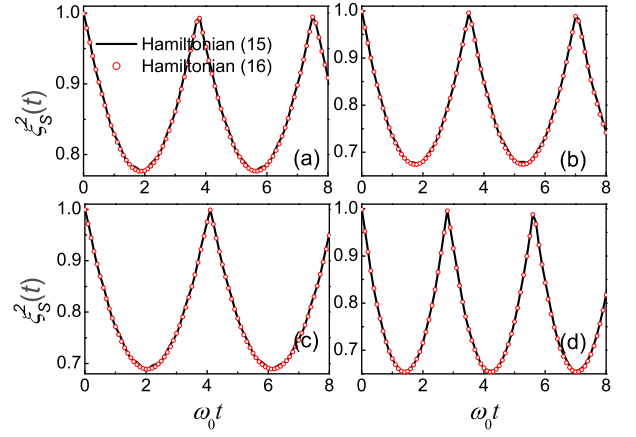

FIG. 2: (Color online). Numerical plots of the time-dependent spin squeezing factors $\xi_S^2(t)$ of both the Hamiltonians (15) and (16), with the same initial states $|J_z = -j\rangle$. In (a) and (b), $\omega_A/\omega_0 = 200$, $\omega_B/\omega_0 = \pm 200$ ["+" for (a) and "−" for (b)], $\lambda_1/\omega_0 = 2$, $\lambda_2/\omega_0 = 1$, and $N = 15$. In (c) and (d), $\omega_A/\omega_0 = 200$, $\omega_B/\omega_0 = \pm 200$ ["+" for (c) and "−" for (d)], $\lambda_1/\omega_0 = 1$, $\lambda_2/\omega_0 = 2$, and $N = 20$.

are the effective atomic resonant frequency and the effective frequencies of two photon modes a and b, respectively, and

$$\lambda_{r_i} = \frac{1}{2} \frac{g_{r_i} \Omega_{r_i}}{\Delta_{r_i}}, \lambda_{s_i} = \frac{1}{2} \frac{g_{s_i} \Omega_{s_i}}{\Delta_{s_i}}, (i = 1, 2) \tag{11}$$

are the effective atom-photon coupling strengths.

When choosing $g_{r_i}^2/\Delta_{r_i} = g_{s_i}^2/\Delta_{s_i}$, $\Omega_{r_i} g_{r_i}/\Delta_{r_i} = \Omega_{s_i} g_{s_i}/\Delta_{s_i}$, and $\varphi_{s_i} = -\varphi_{r_i} = \varphi_i$, the Hamiltonian (7) turns into

$$\widetilde{H} = \omega_A a^\dagger a + \omega_B b^\dagger b + \omega_0 J_z + \lambda_1 (a^\dagger + a) \tag{12}$$

$$\times \big(J_+ e^{-i\varphi_1} + J_- e^{i\varphi_1} \big) + \lambda_2 (J_+ e^{-i\varphi_2} + J_- e^{i\varphi_2})(b^\dagger + b),$$

where the effective atom-photon coupling strengths become

$$\lambda_1 = \frac{1}{2} \frac{\Omega_{s_1} g_{s_1}}{\Delta_{s_1}} = \frac{1}{2} \frac{\Omega_{r_1} g_{r_1}}{\Delta_{r_1}}, \tag{13}$$

$$\lambda_2 = \frac{1}{2} \frac{\Omega_{s_2} g_{s_2}}{\Delta_{s_2}} = \frac{1}{2} \frac{\Omega_{r_2} g_{r_2}}{\Delta_{r_2}}. \tag{14}$$

If setting $\varphi_1 = 0$ and $\varphi_2 = -\pi/2$, the Hamiltonian (12) becomes

$$\widetilde{H} = \omega_A a^\dagger a + \omega_B b^\dagger b + \omega_0 J_z \tag{15}$$

$$+ \lambda_1 J_x (a^\dagger + a) + \lambda_2 J_y (b^\dagger + b).$$

The Hamiltonian (15) is our required two-mode Dicke model, based on recent experiments of cavity-assisted Raman transitions [41, 42]. In contrast to the convectional two-mode Dicke model achieved in the two-level atoms,

the Hamiltonian (15) has a distinct property that all parameters can be tuned independently. For example, the effective cavity frequencies ω_A and ω_B depend on the detunings Δ_a and Δ_b, respectively; see Eqs. (9) and (10). Thus, they can range from the positive to the negative. The choice of the different cavity frequencies ω_A and ω_B help us to create a tunable two-axis spin Hamiltonian, as will be shown below. The effective atomic resonant frequency ω_0 can also be controlled by the detuning Δ_1; see Eq. (8). In addition, the effective atom-photon coupling strengths λ_1 and λ_2 can be driven by the Rabi frequencies of Raman lasers; see Eqs. (13) and (14).

D. Generalized two-axis spin Hamiltonian

In the following, we mainly consider the dispersive regime, i.e., $\{|\omega_A|, |\omega_B|\} \gg \{\lambda_1, \lambda_2\}$. In such case, the photons are virtually excited, and we can use the Heisenberg equations of motion [44], $\dot{a} = -i(\lambda_1 J_x + \omega_A a) = 0$ and $\dot{b} = -i(\lambda_2 J_y + \omega_B b) = 0$, to obtain $a = -\lambda_1 J_x/\omega_A$ and $b = -\lambda_2 J_y/\omega_B$. As a result, the Hamiltonian (15) becomes

$$H = q(J_x^2 + \chi J_y^2) + \omega_0 J_z, \qquad (16)$$

where

$$q = -\frac{\lambda_1^2}{\omega_A}, \qquad (17)$$

$$\chi = \frac{\omega_A \lambda_2^2}{\omega_B \lambda_1^2}. \qquad (18)$$

In the Hamiltonian (16), the parameter q determines the nonlinear spin-spin interaction J_x^2 induced by the virtual photon, and the dimensionless parameter χ reflects the ratio between the different nonlinear spin-spin interactions J_x^2 and J_y^2. Due to existence of these nonlinear spin-spin interactions with the dimensionless parameter χ and the effective atomic resonant frequency ω_0, here we call the Hamiltonian (16) as a generalized two-axis spin Hamiltonian. In addition, equations (8), (17), and (18) show clearly that all the parameters, including the interaction strength q, the dimensionless parameter χ, and the effective atomic resonant frequency ω_0, can also be tuned independently in experiments.

When chosen reasonable parameters, the generalized two-axis spin Hamiltonian (16) can reduce to some well-studied Hamiltonians. For example, when $\chi > 0$, the Hamiltonian (16) is a standard Lipkin-Meshkov-Glick model [45–47]. When $\omega_0 = 0$, the Hamiltonian (16) reduces to a generalized two-axis twisting Hamiltonian $H_{\mathrm{GTAT}} = q(J_x^2 + \chi J_y^2)$. If further setting $\chi = -1$, a standard two-axis twisting Hamiltonian $H_{\mathrm{TAT}} = q(J_x^2 - J_y^2)$ is derived. Finally, when $\chi = 0$, the Hamiltonian (16) turns into a generalized one-axis twisting Hamiltonian $H_{\mathrm{GOAT}} = q J_x^2 + \omega_0 J_z$ [48], which reduces to the standard one-axis twisting Hamiltonian $H_{\mathrm{OAT}} = q J_x^2$ for
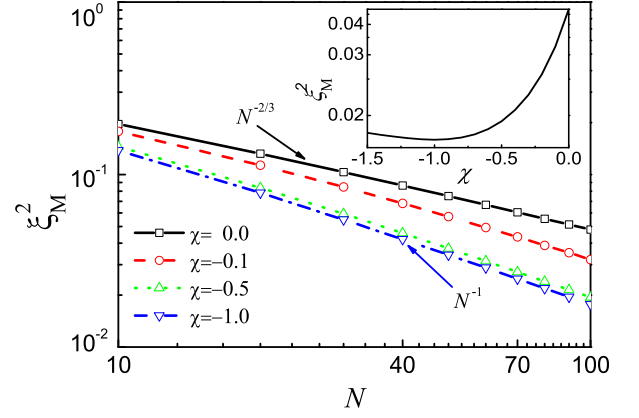

FIG. 3: (Color online). Numerical plots of the maximal squeezing factors ξ_{M}^2 as a function of the atomic number N for the different dimensionless parameters χ. Insert: Numerical plot of the maximal squeezing factor ξ_{M}^2 as a function of the dimensionless parameter χ, when the atomic number is chosen as $N = 100$. In both subfigures, the initial states are chosen as $|J_z = -j\rangle$.

$\omega_0 = 0$. These results implies that the Hamiltonian (16) has an important application in achieving the required spin squeezing.

Notice that when $\omega_A < 0$, the effective spin-spin interaction strength $q > 0$. Thus, we can use the initial state $|J_z = -j\rangle$ to discuss spin squeezing of the generalized two-axis spin Hamiltonian (16). This initial state $|J_z = -j\rangle$ can be easily prepared in experiments. In addition, by combined with the effective atomic resonant frequency ω_0, the dimensionless parameter χ plays an important role in spin squeezing, as will be shown.

III. SPIN SQUEEZING FACTOR

In order to investigate spin squeezing, it is very necessary to consider the following time-dependent squeezing factor [1]:

$$\xi_S^2(t) = \frac{4}{N} \min\left[\Delta J_{\vec{n}_\perp}^2(t)\right], \qquad (19)$$

where $\vec{n}_\perp$ refers to an axis, which is perpendicular to the mean-spin direction $\vec{n}_0 = \vec{J}/|J|$ with $|J| = \sqrt{\langle J_x\rangle^2 + \langle J_y\rangle^2 + \langle J_z\rangle^2}$, and $\Delta A^2 = \langle A^2\rangle - \langle A\rangle^2$ is the standard deviation. If $\left|\xi_S^2(t)\right| < 1$, the spin state is squeezed, and vice versa.

In the spherical coordinates, $\vec{n}_0 = (\sin\theta\cos\varphi, \sin\theta\sin\varphi, \cos\theta)$, where $\theta = \arccos(\langle J_z\rangle/|J|)$, and $\varphi = \arccos(\langle J_x\rangle/|J|\sin\theta)$ for $\langle J_y\rangle > 0$ or $\varphi = 2\pi - \arccos(\langle J_x\rangle/|J|\sin\theta)$ for $\langle J_y\rangle \leq 0$. Two orthogonal bases are given by $\vec{n}_1 = (-\sin\varphi, \cos\varphi, 0)$ and $\vec{n}_2 = (-\cos\theta\cos\varphi, \cos\theta\sin\varphi, -\sin\theta)$. Thus, $J_{\vec{n}_{1,2}} = \vec{J}\cdot\vec{n}_{1,2}$, $J_{\vec{n}_\perp} = J_{\vec{n}_1}\cos\phi + J_{\vec{n}_2}\sin\phi$, and
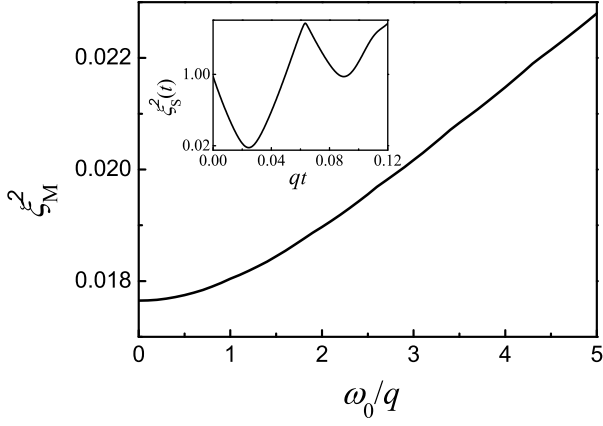
FIG. 4: (Color online). Numerical plot of the maximal squeezing factor ξ_M^2 as a function of the effective atomic resonant frequency ω_0. Insert: Numerical plot of the time-dependent squeezing factor $\xi_S^2(t)$. In both subfigures, the initial states, the dimensionless parameter, and the atomic number are chosen as $|J_z = -j\rangle$, $\chi = -1$, and $N = 100$, respectively.
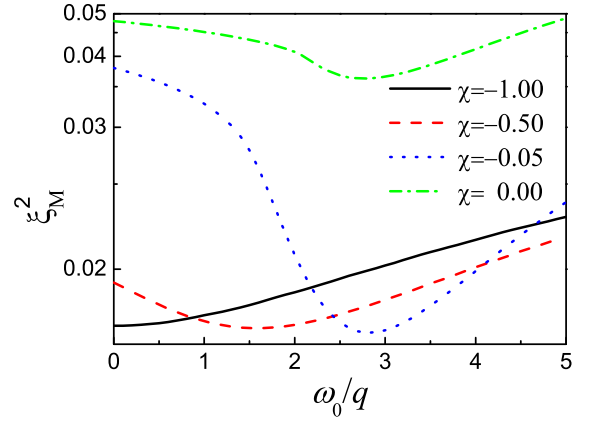

FIG. 5: (Color online). Numerical plots of the maximal squeezing factors ξ_M^2 as a function of the effective atomic resonant frequency ω_0 for the different dimensionless parameters χ. The initial state and the atomic number are chosen as $|J_z = -j\rangle$ and $N = 100$, respectively.

$\min(\Delta J_{\vec{n}_\perp}^2)$ could be achieved when ϕ varies from 0 to 2π in the plane that is perpendicular to the mean-spin direction $\vec{n}_0$. It should be noticed that in experiments, the maximal squeezing factor ξ_M^2 is usually measured [2, 3]. Thus, in the following discussions, we mainly focus on this physical quantity.

Before proceeding, we check the validity of the Hamiltonian (16), when the initial state is chosen as $|J_z = -j\rangle$. For the generalized two-axis spin Hamiltonian, it is very hard to obtain analytical result of the spin squeezing factor $\xi_S^2(t)$ [2]. In Fig. 2, we numerically plot the corresponding spin squeezing factors $\xi_S^2(t)$ of the Hamiltonians (15) and (16). It can be seen clearly that the results of the Hamiltonian (16) are almost identical to those of the Hamiltonian (15). Therefore, we will apply the Hamiltonian (16) to discuss the experimentally-measurable maximal squeezing factor ξ_M^2 in the rest of this paper.

IV. MAXIMAL SQUEEZING FACTOR

We first address a simple case without the effective atomic resonant frequency ($\omega_0 = 0$), in which the generalized two-axis spin Hamiltonian (16) reduces to the generalized two-axis twisting Hamiltonian $H_{GTAT} = q(J_x^2 + \chi J_y^2)$. In Fig. 3, we numerically plot the maximal squeezing factor ξ_M^2 of the Hamiltonian H_{GTAT} as a function of the atomic number N for the different dimensionless parameters χ, when the initial state is chosen as $|J_z = -j\rangle$. This figure shows clearly that when $\chi = 0$, the generalized two-axis twisting Hamiltonian H_{GTAT} becomes the standard one-axis twisting Hamiltonian $H_{OAT} = qJ_x^2$, whose maximal squeezing factor ξ_M^2 scales as $N^{-2/3}$ [1]. When increasing the dimensionless parameter χ, the maximal squeezing factor ξ_M^2 decreases, i.e., spin squeezing is enhanced. In particular, when $\chi = -1$, the Hamiltonian H_{GTAT} turns into the standard two-axis twisting Hamiltonian $H_{TAT} = q(J_x^2 - J_y^2)$, whose maximal squeezing factor ξ_M^2 scales as N^{-1} [1], as expected. In addition, the maximal squeezing factor ξ_M^2 as a function of the dimensionless parameter χ is also plotted in the insert part of Fig. 3. This figure shows that $\chi = -1$ is an optimal point to achieve the maximal squeezing factor ξ_M^2 of the generalized two-axis twisting Hamiltonian H_{GTAT}.

In real experiments, the effective atomic resonant frequency ω_0 always exists. In Fig. 4, we numerically plot the maximal squeezing factor ξ_M^2 of the Hamiltonian $H = q(J_x^2 - J_y^2) + \omega_0 J_z$ as a function of the effective atomic resonant frequency ω_0, when the the initial state is chosen as $|J_z = -j\rangle$. It can be seen from this figure that with the increasing of the effective atomic resonant frequency ω_0 in the standard two-axis twisting Hamiltonian H_{TAT}, the maximal squeezing factor ξ_M^2 increases, i.e., spin squeezing is reduced.

From the above discussions, we argue that when increasing the dimensionless parameter χ (from $\chi = -1$) or introducing the effective atomic resonant frequency ω_0 in the standard two-axis twisting Hamiltonian H_{TAT}, the maximal squeezing factor ξ_M^2 increases, i.e., spin squeezing is reduced. Surprisingly, when we control these two parameters simultaneously, spin squeezing can be enhanced largely. To see this clearly, in Fig. 5 we numerically plot the maximal squeezing factors ξ_M^2 of the generalized two-axis spin Hamiltonian (16), i.e., $H = q(J_x^2 + \chi J_y^2) + \omega_0 J_z$, as a function of the effective atomic resonant frequency ω_0 for the different dimensionless parameters χ, when the initial state is chosen as $|J_z = -j\rangle$. This figure shows that in the case of $\chi = -0.05$ or $\chi = -0.5$, when increasing the effective atomic resonant frequency ω_0, the maximal squeezing factor ξ_M^2 first de-

creases largely and then increases, i.e., spin squeezing is first enhanced largely and then reduced. For the generalized one-axis twisting model $H_{\text{GOAT}} = qJ_x^2 + \omega_0 J_z$, the maximal squeezing factor ξ_{M}^2 has a similar behavior (see green dash-dot line in Fig. 5) [48], but its magnitude cannot arrive at the order of our considered two-axis spin Hamiltonian (16) because these two Hamiltonians have different scalings with respect to the atomic number N. These results are benefit for achieving the required spin squeezing in experiments.

V. DISCUSSIONS

Finally, we estimate the relative parameters, based on recent experiments. Two stable ground states are chosen respectively as $|G_0\rangle = |F = 1, m_F = 1\rangle$ and $|G_1\rangle = |F = 2, m_F = 2\rangle$ of ultracold rubidium 87 atoms, where F is the total angular momentum and m_F is the magnetic quantum number. It means that the atomic decay rate is $\gamma/2\pi = 3.0$ MHz, which is the same order as the photonic decay rate $\kappa/2\pi = 1.3$ MHz [41, 42]. In such system, the atom-photon coupling strengths can reach $g_{s_1}/2\pi = 20$ MHz and $g_{s_2}/2\pi = 15$ MHz, respectively. When $\Omega_{s_1}/2\pi = 20$ MHz and $\Delta_{s_1}/2\pi = 100$ MHz, which is responsible for deriving Eq. (11), $\lambda_1/2\pi = 2$ MHz, and thus $q/2\pi = 0.2$ MHz for $\omega_A/2\pi = -20$ MHz. This choice of the detuning ω_A also satisfies the dispersive condition, which is a key condition to realize our generalized two-axis spin Hamiltonian (16). For the dimensionless parameter χ, it can be easily controlled by tuning both the detuning ω_B and the Rabi frequency Ω_{s_2}. When $N = 100$, numerical result shows that the shortest time for generating the maximal squeezing factor ξ_{M}^2 is about $t_m \simeq 20$ ns [see, for example, in the insert part of Fig. 4], which is shorter than both the atomic and photonic life-times γ^{-1} and κ^{-1}. With the increasing of the atomic number N and the atom-photon coupling strength g_{s_1}, t_m becomes shorter and shorter. This indicates that our proposal can be accessible in the current experimental setups.

VI. CONCLUSIONS

In summary, we have proposed an experimentally-feasible system, in which an ensemble of ultracold six-level atoms interacts with two quantized cavity fields and two pairs of Raman lasers, to realize a generalized two-axis spin Hamiltonian $H = q(J_x^2 + \chi J_y^2) + \omega_0 J_z$. We have numerically calculated the experimentally-measurable maximal squeezing factor and revealed that when $\omega_0 = 0$ and $\chi = -1$, the maximal squeezing factor ξ_{M}^2 scales as N^{-1}. More importantly, we have found that by combined with the dimensionless parameter $\chi(> -1)$, the effective atomic resonant frequency ω_0 can enhance spin squeezing largely. Our results are benefit for achieving the required spin squeezing in experiments, and have a potential application in quantum information and quantum metrology.

VII. ACKNOWLEDGEMENTS

[1] M. Kitagawa and M. Ueda, *Squeezed spin states*, Phys. Rev. A **47**, 5138 (1993).

[2] J. Ma, X. Wang, C. P. Sun, and F. Nori, *Quantum spin squeezing*, Phys. Rep. **509**, 89 (2011).

[3] N. P. Robins, P. A. Altin, J. E. Debs, and J. D. Close, *Atom lasers: production, properties and prospects for precision inertial measurement*, Phys. Rep. **529**, 265 (2013).

[4] L. -M. Duan, A. Sørensen, J. I. Cirac, and P. Zoller, *Squeezing and entanglement of atomic beams*, Phys. Rev. Lett. **85**, 3991 (2000).

[5] A. Sørensen, L. -M. Duan, J. I. Cirac, and P. Zoller, *Many-particle entanglement with Bose-Einstein condensates*, Nature (London) **409**, 63 (2001).

[6] R. J. Sewell, M. Koschorreck, M. Napolitano, B. Dubost, N. Behbood, and M. W. Mitchell, *Magnetic sensitivity beyond the projection noise limit by spin squeezing*, Phys. Rev. Lett. **109**, 253605 (2012).

[7] G. Santarelli, P. Laurent, P. Lemonde, A. Clairon, A. G. Mann, S. Chang, A. N. Luiten, and C. Salomon, *Quantum projection noise in an atomic fountain: a high stability cesium frequency standard*, Phys. Rev. Lett. **82**, 4619 (1999).

[8] K. Hammerer, A. S. Sørensen, and E. S. Polzik, *Quantum interface between light and atomic ensembles*, Rev. Mod. Phys. **82**, 1041 (2010).

[9] K. Helmerson and L. You, *Creating massive entanglement of Bose-Einstein condensed atoms*, Phys. Rev. Lett. **87**, 170402 (2001).

[10] I. Bouchoule and K. Mølmer, *Spin squeezing of atoms by the dipole interaction in virtually excited Rydberg states*, Phys. Rev. A **65**, 041803 (2002).

[11] M. Zhang, K. Helmerson, and L. You, *Entanglement and spin squeezing of Bose-Einstein-condensed atoms*, Phys. Rev. A **68**, 043622 (2003).

[12] Y. C. Liu, Z. F. Xu, G. R. Jin, and L. You, *Spin squeezing: transforming one-axis twisting into two-axis twisting*, Phys. Rev. Lett. **107**, 013601 (2011).

[13] C. Shen and L. M. Duan, *Efficient spin squeezing with optimized pulse sequences*, Phys. Rev. A **87**, 051801 (2013).

[14] J. Y. Zhang, X. F. Zhou, G. C. Guo, and Z. W. Zhou, *Dy-

namical spin squeezing via a higher-order Trotter-Suzuki approximation, Phys. Rev. A **90**, 013604 (2014).

[15] W. Huang, Y.-L. Zhang, C.-L. Zou, X.-B. Zou, and G.-C. Guo, *Two-axis spin squeezing of two-component BEC via a continuous driving*, arXiv: 1412.5635.

[16] R. N. Deb, M. Sebawe Abdalla, S. S. Hassan, and N. Nayak, *Spin squeezing and entanglement in a dispersive cavity*, Phys. Rev. A **73**, 053817 (2006).

[17] A. E. B. Nielsen and K. Mølmer, *Atomic spin squeezing in an optical cavity*, Phys. Rev. A **77**, 063811 (2008).

[18] M. H. Schleier-Smith, I. D. Leroux, and V. Vuletić, *Squeezing the collective spin of a dilute atomic ensemble by cavity feedback*, Phys. Rev. A **81**, 021804 (2010).

[19] I. D. Leroux, M. H. Schleier-Smith, and V. Vuletić, *Implementation of cavity squeezing of a collective atomic spin*, Phys. Rev. Lett. **104**, 073602 (2010).

[20] Z. Chen, J. G. Bohnet, S. R. Sankar, J. Dai, and J. K. Thompson, *Conditional spin squeezing of a large ensemble via the vacuum Rabi splitting*, Phys. Rev. Lett. **106**, 133601 (2011).

[21] E. D. Torre, J. Otterbach, E. Demler, V. Vuletić, and M. Lukin, *Dissipative preparation of spin squeezed atomic ensembles in a steady state*, Phys. Rev. Lett. **110**, 120402 (2013).

[22] Z. Chen, J. G. Bohnet, J. M. Weiner, K. C. Cox, and J. K. Thompson, *Cavity-aided nondemolition measurements for atom counting and spin squeezing*, Phys. Rev. A **89**, 043837 (2014).

[23] L. Yu, J. Fan, S. Zhu, G. Chen, S. Jia, and F. Nori, *Creating a tunable spin squeezing via a time-dependent collective atom-photon coupling*, Phys. Rev. A **89**, 023838 (2014).

[24] A. Messina, S. Maniscalco, and A. Napoli, *Interaction of bimodal fields with few-level atoms in cavities and traps*, J. Mod. Phys. **50**, 1 (2003).

[25] M. Mariantoni, F. Deppe, A. Marx, R. Gross, F. K. Wilhelm, and E. Solano, *Two-resonator circuit quantum electrodynamics: a superconducting quantum switch*, Phys. Rev. B **78**, 104508 (2008).

[26] M. Mariantoni, H. Wang, R. C. Bialczak, M. Lenander, E. Lucero, M. Neeley, A. D. O'Connell, D. Sank, M. Weides, J.Wenner, T. Yamamoto, Y. Yin, J. Zhao, J. M. Martinis, and A. N. Cleland, *Photon shell game in three-resonator circuit quantum electrodynamics*, Nat. Phys. **7**, 287 (2011).

[27] D. J. Egger and F. K. Wilhelm, *Multimode circuit quantum electrodynamics with hybrid metamaterial transmission lines*, Phys. Rev. Lett. **111**, 163601 (2013).

[28] A. Wickenbrock, M. Hemmerling, G. R. M. Robb, C. Emary, and F. Renzoni, *Collective strong coupling in multimode cavity QED*, Phys. Rev. A **87**, 043817 (2013).

[29] D. O. Krimer, M. Liertzer, S. Rotter, and H. E. Tureci, *Route from spontaneous decay to complex multimode dynamics in cavity QED*, Phys. Rev. A **89**, 033820 (2014).

[30] J. Larson and S. Levin, *Effective Abelian and non-Abelian gauge potentials in cavity QED*, Phys. Rev. Lett. **103**, 013602 (2009).

[31] J. Larson, *Analog of the spin-orbit-induced anomalous Hall effect with quantized radiation*, Phys. Rev. A **81**, 051803 (2010).

[32] S. Gopalakrishnan, B. L. Lev, and P. M. Goldbart, *Emergent crystallinity and frustration with Bose–Einstein condensates in multimode cavities*, Nat. Phys. **5**, 845 (2009).

[33] S. Gopalakrishnan, B. L. Lev, and P. M. Goldbart, *Atom-light crystallization of BECs in multimode cavities: nonequilibrium classical and quantum phase transitions, emergent lattices, supersolidity, and frustration*, Phys. Rev. A **82**, 043612 (2010).

[34] S. Gopalakrishnan, B. L. Lev, and P. M. Goldbart, *Frustration and glassiness in spin models with cavity-mediated interactions*, Phys. Rev. Lett. **107**, 277201 (2011).

[35] P. Strack and S. Sachdev, *Dicke quantum spin glass of atoms and photons*, Phys. Rev. Lett. **107**, 277202 (2011).

[36] M. Buchhold, P. Strack, S. Sachdev, and S. Diehl, *Dicke-model quantum spin and photon glass in optical cavities: nonequilibrium theory and experimental signatures*, Phys. Rev. A **87**, 063622 (2013).

[37] A. Andreanov and M. Müller, *Long-range quantum Ising spin glasses at T=0: gapless collective excitations and universality*, Phys. Rev. Lett. **109**, 177201 (2012).

[38] J. Fan, Z. Yang, Y. Zhang, J. Ma, G. Chen, and S. Jia, *Hidden continuous symmetry and Nambu-Goldstone mode in a two-mode Dicke model*, Phys. Rev. A **89**, 023812 (2014).

[39] R. Guzmán, J. C. Retamal, E. Solano, and N. Zagury, *Field squeeze operators in optical cavities with atomic ensembles*, Phys. Rev. Lett. **96**, 010502 (2006).

[40] A. S. Parkins, E. Solano, and J. I. Cirac, *Unconditional two-mode squeezing of separated atomic ensembles*, Phys. Rev. Lett. **96**, 053602 (2006).

[41] K. Baumann, C. Guerlin, F. Brennecke, and T. Esslinger, *Dicke quantum phase transition with a superfluid gas in an optical cavity*, Nature (London) **464**, 1301 (2010).

[42] M. P. Baden, K. J. Arnold, A. L. Grimsmo, S. Parkins, and M. D. Barrett, *Realization of the Dicke model using cavity-assisted Raman transitions*, Phys. Rev. Lett. **113**, 020408 (2014).

[43] F. Dimer, B. Estienne, A. S. Parkins, and H. J. Carmichael, *Proposed realization of the Dicke-model quantum phase transition in an optical cavity QED system*, Phys. Rev. A **75**, 013804 (2007).

[44] J. Larson, *Circuit QED scheme for the realization of the Lipkin-Meshkov-Glick model*, EPL **90**, 54001 (2010).

[45] H. J. Lipkin, N. Meshkov, and N. Glick, *Validity of many-body approximation methods for a solvable model: (I). exact solutions and perturbation theory*, Nucl. Phys. A **62**, 188 (1965).

[46] H. J. Lipkin, N. Meshkov, and N. Glick, *Validity of many-body approximation methods for a solvable model: (II). linearization procedures*, Nucl. Phys. A **62**, 199 (1965).

[47] H. J. Lipkin, N. Meshkov, and N. Glick, *Validity of many-body approximation methods for a solvable model: (III). diagram summations*, Nucl. Phys. A **62**, 211 (1965).

[48] C. K. Law, H. T. Ng, and P. T. Leung, *Coherent control of spin squeezing*, Phys. Rev. A **63**, 055601 (2001).